RSC Advances

PAPER

View Article Online
View Journal | View Issue

Cite this: *RSC Adv.*, 2024, **14**, 39353

Electrochemical reduction method for leaching terbium and cerium from waste phosphors†

Ruixiang Wang,[abc] Piao Xu,[ab] Boyi Xie, *[abc] Chaxiang Liu,[d] Xiaocong Zhong,[abc] Zhongtang Zhang [abc] and Helin Fan[abc]

Rare earth elements are commonly used in various fields due to their unique physical and chemical properties. Waste phosphors represent an important secondary source of rare earth elements, and their recovery is a crucial means of improving the utilization of these resources. When using $FeCl_2$ as a reducing agent to reduce Tb^{4+} and Ce^{4+} from washed phosphors, a large amount of reducing agent is required, and the Fe^{2+} cycle becomes complicated. In this study, the electrochemical reduction process was employed to treat washed phosphors. Under optimum conditions of $FeCl_2$ concentration of 0.10 mol L^{-1}, current density of 100 A m^{-2}, HCl concentration of 3 mol L^{-1}, temperature of 80 °C, L/S ratio of 30 mL g^{-1}, and time of 60 min, the leaching efficiencies of Tb and Ce reached 99.2% and 98.5%, respectively. The apparent activation energies of Tb and Ce were calculated as 17.71 and 18.46 kJ mol^{-1}, respectively, illustrating that the leaching processes of Tb and Ce depend on the diffusion. By applying an external electric field, Fe^{2+} can be recycled in the system, thereby reducing the amount of reducing agent needed and achieving a higher leaching efficiency for Tb and Ce. These results are beneficial for the resource utilization of waste phosphors and have significant implications for the sustainable development of rare earth resources.

Received 2nd September 2024
Accepted 8th December 2024

DOI: 10.1039/d4ra06334a

rsc.li/rsc-advances

1 Introduction

Rare earth elements (REEs) include the lanthanide elements, as well as scandium (Sc) and yttrium (Y), totaling 17 elements.[1] Rare earths are commonly used in various fields due to their unique physical and chemical properties.[2,3] With the increasing demand for rare earths and the continuous exploitation of these resources, the supply is facing a shortage. The recycling and utilization of secondary rare earth resources are an important means to improve the utilization rate of rare earth resources.[4,5]

REEs are most widely used in luminescent materials, especially in the production of tri-color fluorescent lamps, which feature low thermal radiation, customizable light colors, and high light efficiency.[6] The tri-color fluorescent lamps have rapidly developed within the traditional fluorescent lamp industry and quickly became the main light source for indoor lighting.[7,8] However, with the upgrading of lighting products in recent years, various new light sources, such as LED lights, have emerged and replaced traditional tri-color fluorescent lamps.[9] As a result, traditional tri-color fluorescent lamps are gradually being abandoned, and their disposal is often limited to buried or incineration as domestic waste, leading to serious environmental pollution and the waste of rare earth resources.[10,11] Tri-color phosphors, which are an important component of fluorescent lamps, contain significant amounts of REEs and toxic metals that are harmful to the environment.[12] As industrial solid waste containing high-value REEs, these phosphors are abundant, produced in large quantities, and have low disposal costs. The total content of REEs in phosphors can be as high as 23%, which is more than 15 times that of the lowest industrial grade of primary rare earth ore.[13,14] As the most widely used phosphor system, aluminate phosphors have become the focus of recycling efforts for waste rare earth phosphors.[15]

The recycling of waste phosphors mainly includes two methods: physical and chemical.[16,17] The physical method refers to the separation based on the differences in magnetic susceptibility, hydrophobicity, density, and particle size among different phosphors. However, the physical method cannot efficiently recover REEs.[18–20] Chemical methods, including extraction, acid leaching, alkali roasting, and mechanical activation, have become the primary methods for recycling rare earths.[21–23] Acid leaching can effectively extract Y and Eu from red powder, while it is difficult to extract Tb and Ce from green and blue powders due to the stable Al–Mg spinel structure.[24] Therefore, alkali roasting pretreatment is usually used

[a]School of Metallurgical Engineering, Jiangxi University of Science and Technology, Ganzhou 341000, China. E-mail: xieboyi90@163.com
[b]Ganzhou Engineering Technology Research Center of Green Metallurgy and Process Intensification, Ganzhou 341000, China
[c]Key Laboratory of Ionic Rare Earth Resources and Environment, Ministry of Natural Resources, Ganzhou 341000, China
[d]Ganzhou Polytechnic, Ganzhou 341000, China

† Electronic supplementary information (ESI) available. See DOI: https://doi.org/10.1039/d4ra06334a

employed before acid leaching to destroy the Al–Mg spinel structure in the waste phosphors.[25] Wu *et al.*[26] used a Na_2O_2 roasting method to recover REEs from waste phosphors. At a roasting temperature of 650 °C for 50 min, 99.9% of REEs were recovered. Although alkali roasting can destroy the structure of Al–Mg spinel in waste phosphors, the REEs of Tb and Ce are oxidized to a high valence state after alkali roasting, while high-valence REEs hardly dissolve in acid, resulting in low rare earth leaching efficiency.[27] Liang *et al.*[28] inhibited the oxidation of Tb and Ce by adding reductive iron powder during alkali roasting. Under the conditions of a mass ratio of reductive iron powder to waste rare earth phosphor of 1 : 200, an alkali to phosphor mass ratio of 2 : 1, an alkali fusion temperature of 700 °C, and an alkali fusion time of 3 h, the total leaching efficiency of REEs reached as high as 99.35%.

In our previous research, NaOH roasting and reduction leaching were used in the treatment of waste phosphors. $FeCl_2$ served as the reducing agent in the reduction leaching process, reducing the high-valence REEs of Tb and Ce to low-valence forms, thereby improving the leaching efficiency of REEs.[29] However, the amount of the reducing agent $FeCl_2$ required is substantial, and Fe^{2+} can only be recycled through a series of processes, such as extraction. Electrochemical reduction is a method that provides electrons to ions or molecules in a liquid through an electrode and a solid/liquid interface, allowing them to undergo a reduction reaction.[30] In recent years, the electrochemical reduction method has been widely used in the recovery of valuable metals, which benefits the improvement of leaching efficiency and reduces the amount of reagents needed.[31,32] Yang *et al.*[33] demonstrated an improvement in the leaching efficiency of Li, Ni, Co, and Mn from waste lithium-ion batteries through an electric field-enhanced leaching process. Under the conditions of 2.0 mol per L H_2SO_4, 0.1 mol per L $FeSO_4$, 20 g per L NaCl, a current density of 200 A m^{-2}, an S/L ratio 80 g L^{-1}, a leaching temperature of 80 °C, and a leaching time >60 min, the leaching efficiencies of Li, Ni, Co, Mn reached up to 98%, 97%, 97%, and 93%, respectively. However, there are no relevant reports on the application of the electrochemical reduction method in waste phosphors.

Based on the above, the electrochemical reduction method is employed to treat the waste phosphors. The direct recycling of the reducing agent Fe^{2+} is achieved, and the leaching efficiencies of Tb and Ce are improved. In this text, the electrochemical reaction process and mechanism are investigated in detail. These results are beneficial for the resource utilization of waste phosphors and have significant implications for the sustainable development of rare earth resources.

2 Experimental

2.1 Pretreatment of waste phosphors

The waste phosphors used in the experiments were obtained from fluorescent lamps (YZ32RR26, 32 W), supplied by Optonix new material company (Guangdong, China). The chemical composition of the waste phosphors is shown in Table 1. The waste phosphors were composed of Y_2O_3, Eu_2O_3, Tb_4O_7, CeO_2, Al_2O_3, MgO, and BaO. First, the waste phosphors were roasted with NaOH under the following conditions: a NaOH/sample mass ratio of 2.5 : 1, a roasting temperature of 900 °C, and a roasting time of 120 min. Then, the waste phosphors were washed with water under the following conditions: an L/S ratio of 50 : 1, a washing temperature of 60 °C, and a washing time of 20 min. Finally, the washed phosphors were obtained for the subsequent electrochemical reduction leaching.

Table 1 Chemical composition of the waste phosphors (wt%)

Compound	Al_2O_3	BaO	MgO	Y_2O_3	Eu_2O_3	Tb_4O_7	CeO_2	Others
Content	56.49	3.70	3.95	11.30	1.84	5.72	8.33	8.67

2.2 Electrochemical reduction leaching of washed phosphors

The electrochemical reduction leaching experiment was performed in a beaker immersed in a thermostatically controlled water bath with magnetic stirring. The experimental apparatus is illustrated in Fig. 1. Both the anode and cathode electrodes were made of graphite and powered by a DC power supply. The washed phosphor samples and $FeCl_2$ were added to the beaker, and a certain amount of hydrochloric acid was poured in. The power supply was then turned on, and the current was adjusted to the desired value according to the current density. Finally, the filtrate was collected for analysis of the REE concentrations.

The leaching efficiency of Tb (or Ce) can be calculated as follows:

$$\eta_i = \frac{C_i \times V}{m \times w_i} \quad (1)$$

where η_i is the leaching efficiency of Tb (or Ce) (%), C_i is the concentration of Tb (or Ce) in the leaching solution (g L^{-1}), V is the volume of the leaching solution (L), m is the weight of the waste phosphors (g), and w_i is the percentage of Tb (or Ce) in the waste phosphors (%).

2.3 Analytical methods

The chemical composition of the waste phosphors was measured using inductively coupled plasma optical emission spectrometry (ICP-OES, iCAP 7400, Thermo Fisher, Germany) after acid digestion. The concentrations of Tb and Ce in the solution were determined by ICP-OES. XRD patterns of the leaching residue were obtained using an X-ray diffractometer (TTRAX-3, Rigaku, Japan) equipped with Cu Kα radiation at 40 kV, 250 mA, and 10° min^{-1}. The microstructures of the leaching residue were characterized using a scanning electron microscope (SEM, Hitachi SU8100, Japan).

3. Results and discussion

3.1 Electrochemical reduction leaching factors influence

3.1.1 Effect of $FeCl_2$ concentration. Fig. 2a shows the effect of $FeCl_2$ concentration on the leaching efficiencies of Tb and Ce. It can be seen from Fig. 2a that as the $FeCl_2$ concentration increased from 0.06 to 0.10 mol L^{-1}, the leaching efficiencies of Tb and Ce increased from 73.1% and 65.3% to 94.1% and

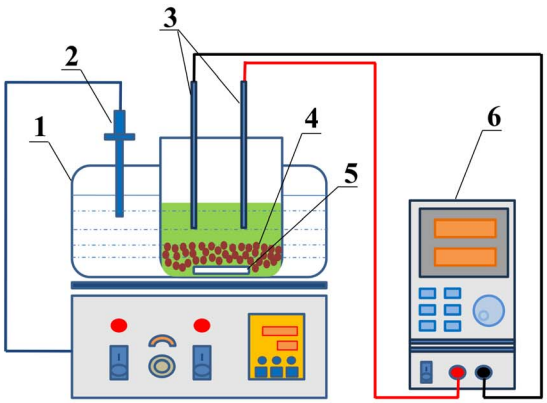

1. Water bath; 2. Thermocouple; 3. Electrodes; 4. Magnetic rotor; 5. Washed phosphor; 6. DC power supply

Fig. 1 Apparatus of the electrochemical reduction leaching experiment.

92.2%, respectively. Due to the reducibility of Fe^{2+}, Tb^{4+} and Ce^{4+} can be reduced to Tb^{3+} and Ce^{3+}, respectively, thus promoting the leaching of Tb and Ce.[29] The related reactions are listed in eqn (2) and (3):

$$Tb_4O_7 + 14HCl + 2FeCl_2 = 4TbCl_3 + 2FeCl_3 + 7H_2O \quad (2)$$

$$CeO_2 + 4HCl + FeCl_2 = CeCl_3 + FeCl_3 + 2H_2O \quad (3)$$

Further increasing the $FeCl_2$ concentration results in only a slight increase in the leaching efficiencies of Tb and Ce. Considering that Fe^{2+} can be recycled in the system, the optimum $FeCl_2$ concentration was chosen to be 0.10 mol L^{-1}.

3.1.2 Effect of current density. The effect of current density on the leaching efficiencies of Tb and Ce is shown in Fig. 2b. The current density significantly affects the Tb and Ce leaching efficiency. When no current was applied, the leaching efficiencies of Tb and Ce were approximately 67.3% and 64.1%, respectively. When the current density was 50 A m^{-2}, the leaching efficiencies of Tb and Ce increased to 88.2% and 81.6%, respectively. Further increasing the current density to 100 A m^{-2} resulted in maximum leaching efficiencies of 97.0% for Tb and 95.3% for Ce. This increase may be attributed to the reduction of newly formed Fe^{3+} back to Fe^{2+} on the cathode surface, which re-engages it in the leaching reaction and thus contributes to the increased REE leaching efficiency.[33] However, with further increases in current density, the leaching efficiency tends to decline. This may be due to the oxidation of Tb^{3+} and Ce^{3+} in the solution to Tb^{4+} and Ce^{4+}, respectively, on the anode surface. Therefore, the suitable current density was 100 A m^{-2}.

3.1.3 Effect of HCl concentration. Fig. 2c shows the effect of HCl concentration on the leaching efficiencies of Tb and Ce. With the increase of HCl concentration, the leaching efficiencies of Tb and Ce initially increased and then remained unchanged. This indicates that there is a critical value for the influence of HCl concentration on the leaching efficiencies of Tb and Ce, which is approximately 3 mol L^{-1}. In a high-acid system, the reduction reaction of Tb and Ce by Fe^{2+} can be enhanced. Moreover, increasing the HCl concentration would also increase the Cl^- concentration. The Cl^- loses electrons at the anode to form Cl_2, which can inhibit the oxidation of Tb^{3+} and Ce^{3+} on the anode surface, thus increasing the leaching efficiency of Tb and Ce.[33] As a result, the optimized HCl concentration was determined to 3 mol L^{-1}.

3.1.4 Effect of temperature. The effect of temperature on the leaching efficiencies of Tb and Ce is shown in Fig. 2d. As the temperature increased from 25 °C to 80 °C, the leaching efficiencies of Tb and Ce increased from 78.2% and 76.1% to 99.2% and 98.5%, respectively. This can be explained by the fact that higher temperatures can accelerate the diffusion of substances in the solution.[27] Moreover, elevated temperatures can enhance the kinetic processes of the reduction reaction, thereby promoting the leaching of Tb and Ce. Considering both the leaching efficiencies of Tb and Ce and economic factors, the optimal temperature appears to be 80 °C.

3.1.5 Effect of L/S ratio. Fig. 2e shows the effect of the L/S ratio on the leaching efficiencies of Tb and Ce. The leaching efficiencies of Tb and Ce increased from 61.3% and 56.9% to 99.2% and 98.5%, respectively, as the L/S ratio increased from 10 to 30 mL g^{-1}. This is because increasing the L/S ratio promotes the effective surface area available for each particle to participate in the reaction, thereby accelerating mass transfer at the liquid–solid interface.[28] When the L/S ratio exceeded 30 mL g^{-1}, the leaching efficiencies of Tb and Ce remained relatively stable. Consequently, the optimum L/S ratio was selected to be 30 mL g^{-1}.

3.1.6 Effect of time. The effect of time on the leaching efficiencies of Tb and Ce is shown in Fig. 2f. As can be seen, extending the time is beneficial for the leaching efficiencies of

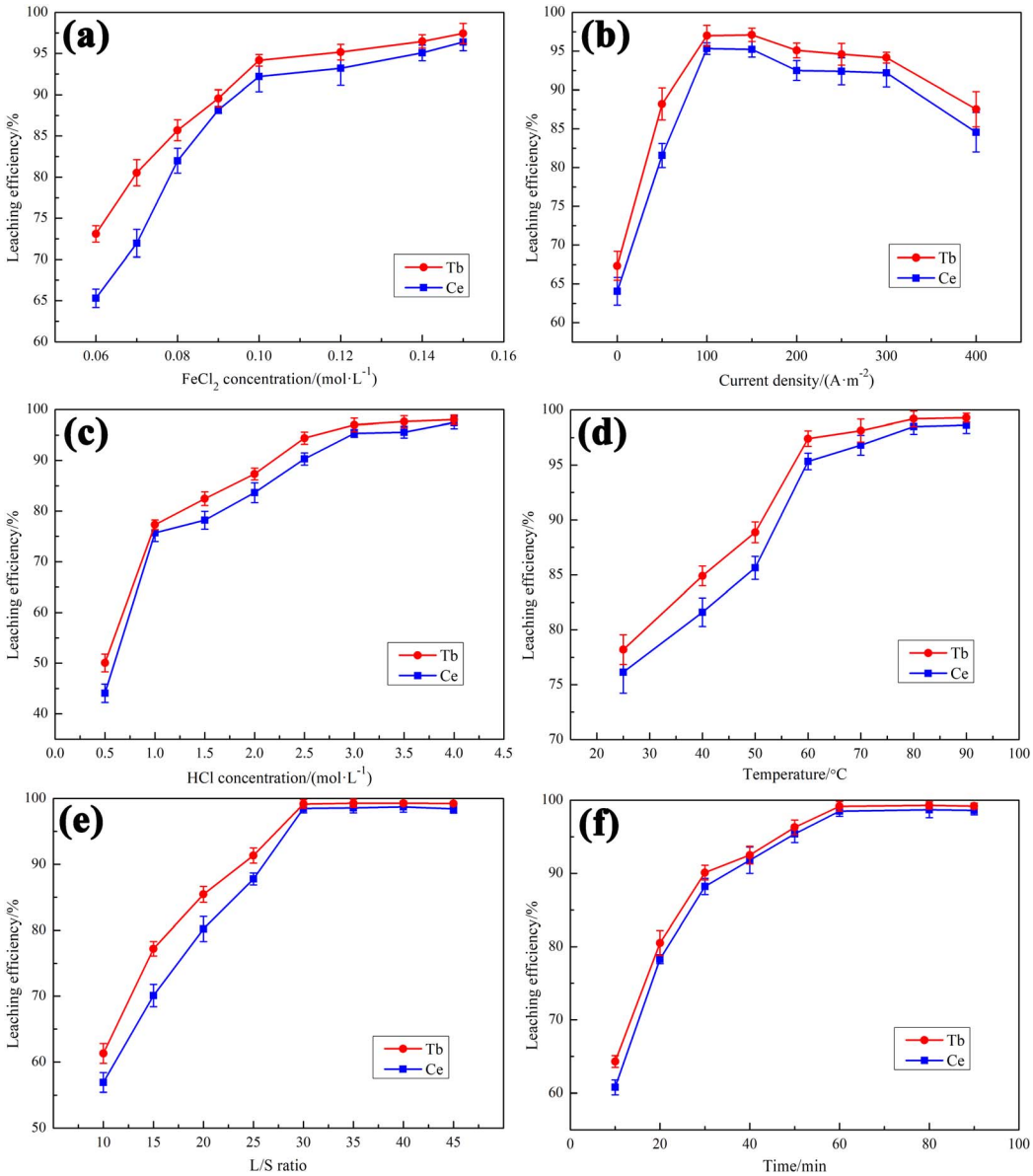

Fig. 2 The effects of the (a) $FeCl_2$ concentration (current density of 300 A m^{-2}, HCl concentration of 3 mol L^{-1}, temperature of 60 °C, L/S ratio of 30 mL g^{-1}, and time of 60 min), (b) current density ($FeCl_2$ concentration of 0.10 mol L^{-1}, HCl concentration of 3 mol L^{-1}, temperature of 60 °C, L/S ratio of 30 mL g^{-1}, and time of 60 min), (c) HCl concentration ($FeCl_2$ concentration of 0.10 mol L^{-1}, current density of 100 A m^{-2}, temperature of 60 °C, L/S ratio of 30 mL g^{-1}, and time of 60 min), (d) temperature ($FeCl_2$ concentration of 0.10 mol L^{-1}, current density of 100 A m^{-2}, HCl concentration of 3 mol L^{-1}, L/S ratio of 30 mL g^{-1}, and time of 60 min), (e) L/S ratio ($FeCl_2$ concentration of 0.10 mol L^{-1}, current density of 100 A m^{-2}, HCl concentration of 3 mol L^{-1}, temperature of 80 °C, and time of 60 min), and (f) time ($FeCl_2$ concentration of 0.10 mol L^{-1}, current density of 100 A m^{-2}, HCl concentration of 3 mol L^{-1}, temperature of 80 °C, and L/S ratio of 30 mL g^{-1}) on the leaching efficiency of Tb and Ce.

both Tb and Ce. This can be explained by the fact that the reduction reaction can be fully completed given sufficient time.[15] Moreover, the oxidized Fe^{3+} can be reduced to Fe^{2+} and re-engage in the leaching reaction with adequate time. When the time exceeded 60 min, the leaching efficiencies of Tb and Ce remained unchanged. Therefore, the appropriate time was determined to be 60 min.

In summary, under the conditions of $FeCl_2$ concentration of 0.10 mol L^{-1}, current density of 100 A m^{-2}, HCl concentration of 3 mol L^{-1}, temperature of 80 °C, L/S ratio of 30 mL g^{-1}, and time of 60 min, the leaching efficiencies of Tb and Ce can reach 99.2% and 98.5%, respectively.

3.2 Kinetics study of Tb and Ce during the leaching process

Kinetic experiments were conducted using the conditions of the leaching process. The leaching of waste phosphors can be regarded as a solid–liquid reaction. The leaching efficiencies of Tb and Ce are plotted as functions of time, as shown in Fig. 3(a) and (b). The shrinking core model was applied in the leaching process, as given in eqn (4) and (5):

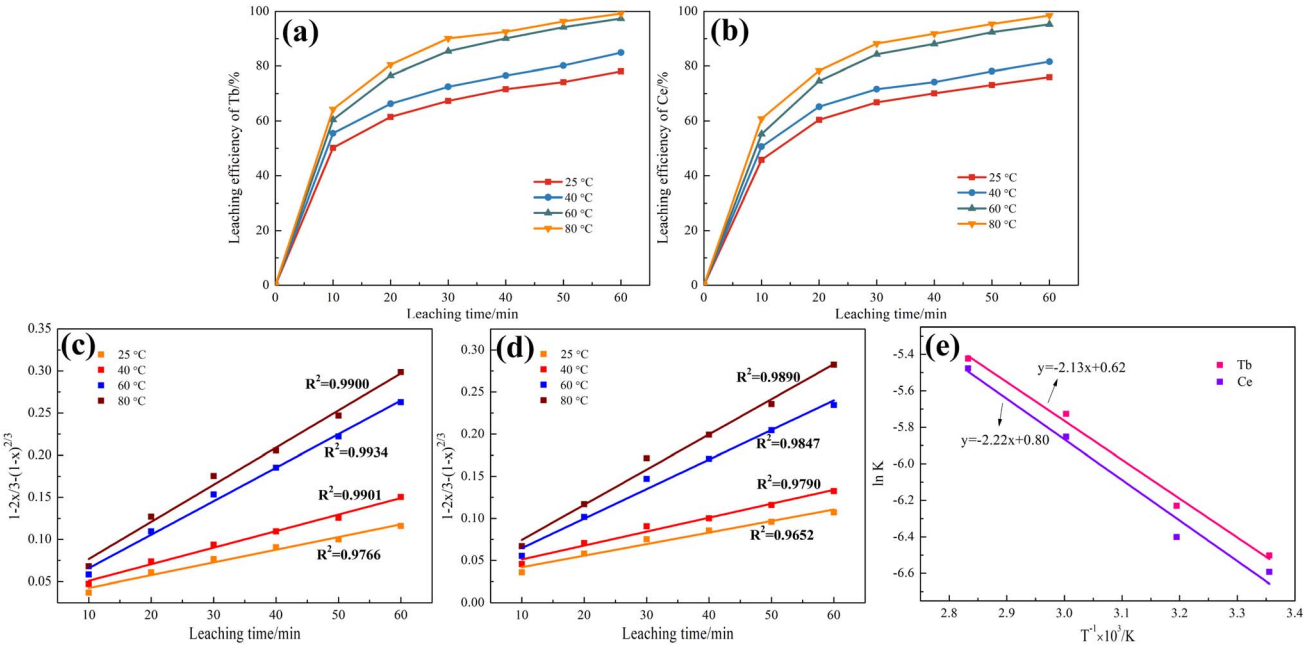

Fig. 3 Leaching efficiencies of (a) Tb and (b) Ce at various temperatures as a function of time, plots of $1 - 2x/3 - (1 - x)^{2/3} - t$ at various temperatures for (c) Tb and (d) Ce, and (e) plot of $\ln k - T^{-1}$.

$$1 - 2x/3 - (1 - x)^{2/3} = kt \quad (4)$$

$$1 - (1 - x)^{1/3} = kt \quad (5)$$

Based on Fig. 3(a) and (b), the relationship between $1 - 2x/3 - (1 - x)^{2/3}$ and t at various temperatures for Tb and Ce were drawn, as shown in Fig. 3(c) and (d). Moreover, the relationship between $1 - (1 - x)^{1/3}$ and t is shown in Fig. S1.† The results indicated that $1 - 2x/3 - (1 - x)^{2/3} - t$ demonstrated the best experimental fit.

Temperature primarily affected the leaching efficiencies of Tb and Ce through the rate constant, which is expressed by the Arrhenius equations (eqn (6)):

$$k = A_0 \times \exp\left(-\frac{E_a}{RT}\right) \quad (6)$$

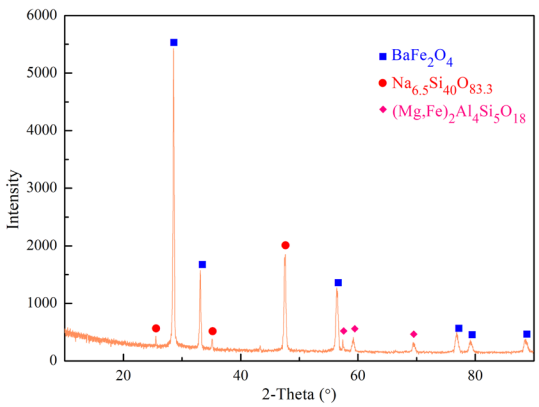

Fig. 4 XRD pattern of the leaching residue.

The plot of $\ln k - T^{-1}$ for Tb and Ce is shown in Fig. 3(e). According to Fig. 3(e), the apparent activation energies of Tb and Ce were calculated as 17.71 and 18.46 kJ mol^{-1}, respectively. The smaller the apparent activation energy, the easier it is for leaching to occur. Therefore, Tb is more easily leached than Ce. In addition, the apparent activation energies of Tb and Ce are both less than 20 kJ mol^{-1}, further illustrating that the Tb and Ce leaching process depended on the diffusion.

3.3 Phase composition of leaching residue

The XRD pattern of the leaching residue is presented in Fig. 4. It can be observed that the leaching residue is primarily composed of $BaFe_2O_4$, $Na_{6.5}Si_{40}O_{83.3}$, and $(Mg,Fe)_2Al_4Si_5O_{18}$. In comparison with the original phosphors shown in Fig. S2,† the main phase of the leaching residue does not contain REEs, which preliminarily indicates that this process effectively leaches REEs from waste phosphors.

Fig. 5 displays the SEM-EDS analysis of the leaching residue. Blocky and spherical particles, presumed to be the different substances, are present in the leaching residue. These substances exhibit no obvious edges or corners and have a dense structure. Moreover, the contents of Y, Eu, Tb, and Ce in locations 1, 2, and 3 are relatively low, primarily consisting of elements such as Na, Mg, Al, Si, Fe, Ba, and O. Therefore, most of the REEs are leached into the solution during the leaching process, which effectively improves the leaching efficiency of the REEs.

3.4 Leaching mechanism

The schematic diagram of the electrochemical reduction leaching mechanism is shown in Fig. 6. In the leaching process,

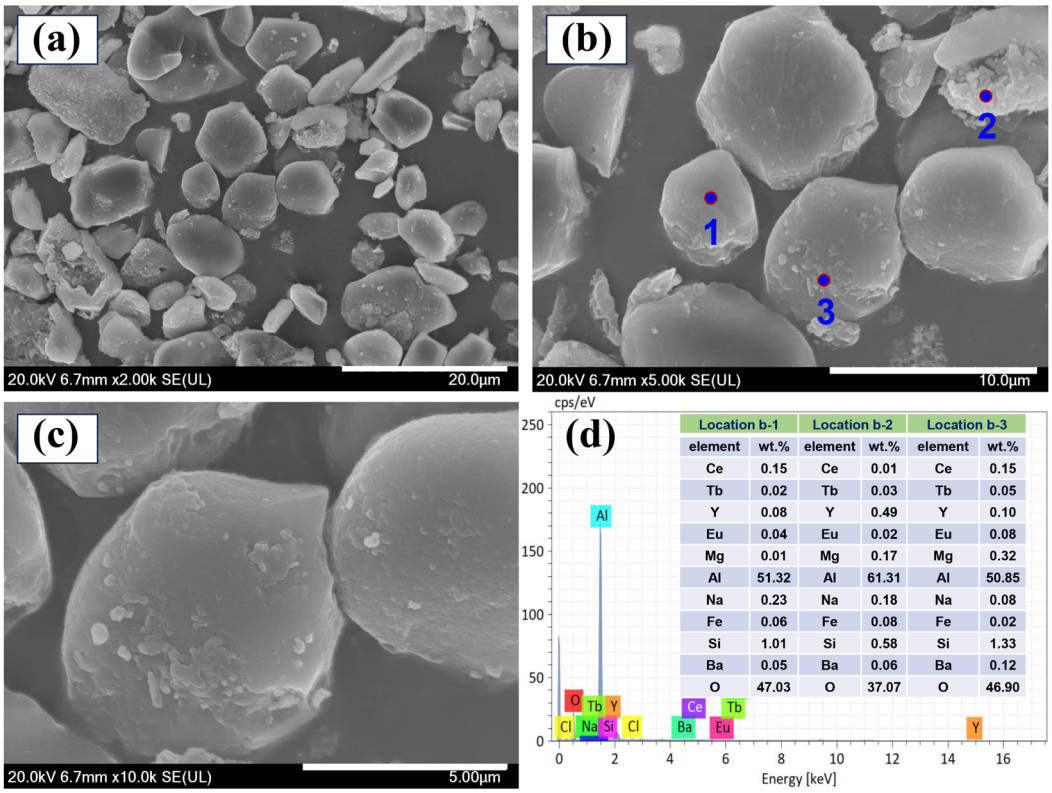

Fig. 5 SEM images of the leaching residue. (a: ×2000; b: ×5000, c: ×10 000), and (d) EDS spectra of the leaching residue. (Points 1, 2, and 3 from b).

Fe^{2+} was used as a reducing agent to react with Tb_4O_7 and CeO_2 in the washed phosphors. The reduction reactions are shown in eqn (2) and (3).

In the reduction reaction, Tb_4O_7 and CeO_2 were reduced to $TbCl_3$ and $CeCl_3$, respectively, while $FeCl_2$ was oxidized to $FeCl_3$. Therefore, Tb and Ce are recovered in the forms of $TbCl_3$ and $CeCl_3$, respectively.

When an external electric field was applied, Fe^{3+} was reduced to Fe^{2+} on the cathode surface, and Fe^{2+} re-participates in the reduction reaction, allowing eqn (2) and (3) to be fully completed. Thus, Fe^{2+} acts as a reducing agent; through the application of the electric field, Fe^{2+} can be recycled in the system, thereby reducing the amount of reducing agent needed and achieving a higher leaching efficiency of Tb and Ce.

Moreover, other reactions could occur in the system. At the anode, Cl^- and H_2O would lose electrons to form Cl_2 and O_2, respectively, as shown in eqn (7) and (8). At the cathode, H^+ would gain electrons to form H_2, as listed in eqn (9).

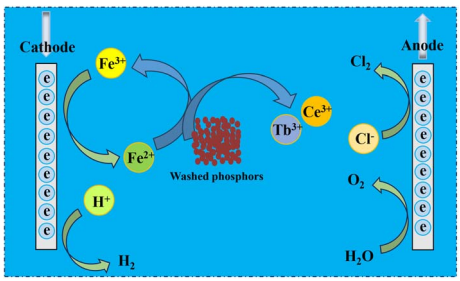

Fig. 6 Schematic diagram of electrochemical reduction leaching mechanism.

$$2Cl^- - 2e = Cl_2 \quad (7)$$

$$2H_2O = 4H^+ + O_2 + 4e \quad (8)$$

$$2H^+ + 2e = H_2 \quad (9)$$

4. Conclusions

In this study, the electrochemical reaction process and mechanism were investigated. The conclusions can be summarized as follows.

(1) The optimum conditions were determined to be a $FeCl_2$ concentration of 0.10 mol L^{-1}, a current density of 100 A m^{-2}, an HCl concentration of 3 mol L^{-1}, a temperature of 80 °C, an L/S ratio of 30 mL g^{-1}, and a time of 60 min. Under these optimum conditions, the leaching efficiencies of Tb and Ce reached 99.2% and 98.5%, respectively.

(2) Leaching kinetics confirmed that the leaching process followed a shrinking core model. The apparent activation energies of Tb and Ce were calculated to be 17.71 and 18.46 kJ mol^{-1}, respectively, illustrating that the leaching process of Tb and Ce depended on the diffusion.

(3) The main phase of the leaching residue does not contain REEs, indicating that most of the REEs are leached into the solution during the leaching process.

(4) Fe^{2+} was used as a reducing agent to react with Tb_4O_7 and CeO_2 present in the washed phosphors. By applying an external electric field, Fe^{2+} can be recycled in the system, thereby reducing the amount of reducing agent needed and achieving a higher leaching efficiency of Tb and Ce.

Author contributions

Ruixiang Wang: writing – original draft, conceptualization, methodology, funding acquisition. Piao Xu: investigation, data curation. Boyi Xie: conceptualization, supervision, writing – review & editing, funding acquisition. Chaxiang Liu: methodology. Xiaocong Zhong: funding acquisition. Zhongtang Zhang: funding acquisition. Helin Fan: data curation.

Conflicts of interest

The authors declare that they have no known competing financial interests or personal relationships that could have appeared to influence the work reported in this paper.

Acknowledgements

This work was supported by the National Natural Science Foundation of China (No. 52064022); the Distinguished Professor Program of Jinggang Scholars in institutions of higher learning, Jiangxi Province; the Jiangxi Provincial Natural Science Foundation (No. 20232BAB214040); the Science and Technology Research Project of Jiangxi Provincial Department of Education (No. GJJ210810); the Training plan for academic and technical leaders of major disciplines in Jiangxi Province (Youth Program; 20212BCJ23006); the Jiangxi University of Science and Technology Landing Project (No. 2021016); and the Ganpo Juncai Support Program Youth Science and Technology Talent Support Project (2024QT06).

References

1 S. Xie, J. Yang, R. Huang, X. Lv, X. Li and X. He, A novel process for the separation and recovery of phosphorus and rare earth elements from associated rare earth phosphate ores, *Sep. Purif. Technol.*, 2024, **340**, 126687, DOI: 10.1016/j.seppur.2024.126687.

2 L. Zhou, S. Kang, J. Yang, X. Wang, H. Yu and Y. Wan, Effect of particlesize on the leaching of a weathered crust elution-deposited rare earth ore, *Hydrometallurgy*, 2023, **222**, 106200, DOI: 10.1016/j.hydromet.2023.106200.

3 X. Chen, J. Chen, J. Li, L. Huang, J. Xu and Y. Xiao, Strengthening rare earth and inhibiting aluminum leaching in magnesium salt-acetic acid compound system from ion-adsorption type rare earth ore, *Sep. Purif. Technol.*, 2024, **334**, 126070, DOI: 10.1016/j.seppur.2023.126070.

4 B. Gao, M. Gan, C. Sun, H. Chen, X. Liu, Q. Liu, Y. Wang, H. Cheng, H. Zhou and Z. Chen, Bioleaching of ion-adsorption rare earth ores by biogenic lixiviants derived from agriculture waste via a cell-free cascade enzymatic process, *Hydrometallurgy*, 2023, **222**, 106189, DOI: 10.1016/j.hydromet.2023.106189.

5 X. He, L. Chen, P. Chen, W. Liu, D. Zhang and T. Yang, Coordination-enhanced extraction of rare earth metals from waste polishing powder and facile preparation of a mesoporous Ce-La oxide, *Chem. Eng. J.*, 2023, **452**, 139265, DOI: 10.1016/j.cej.2022.139265.

6 L. Viana and T. Saint'Pierre, Environmental impact assessment of end-of-life fluorescent lamps in Rio de Janeiro, Brazil, under different recycling rate scenarios, *Chemosphere*, 2023, **340**, 139835, DOI: 10.1016/j.chemosphere.2023.139835.

7 L. Viana, A. Soares, D. Guimarães, W. Rojano and T. Saint'Pierre, A review on environmental concerns and current recycling perspectives highlighting Hg and rare earth elements, *J. Environ. Chem. Eng.*, 2022, **10**(6), 108915, DOI: 10.1016/j.jece.2022.108915.

8 G. Azimi, M. Sauber and J. Zhang, Technoeconomic analysis of supercritical fluid extraction process for recycling rare earth elements from neodymium iron boron magnets and fluorescent lamp phosphors, *J. Cleaner Prod.*, 2023, **422**, 138526, DOI: 10.1016/j.jclepro.2023.138526.

9 L. Castro, H. Gómez-Álvarez, F. González and J. Muñoz, Biorecovery of rare earth elements from fluorescent lamp powder using the fungus Aspergillus niger in batch and semicontinuous systems, *Miner. Eng.*, 2023, **201**, 108215, DOI: 10.1016/j.mineng.2023.108215.

10 N. Dhawan and H. Tanvar, A critical review of end-of-life fluorescent lamps recycling for recovery of rare earth values, *Sustainable Mater. Technol.*, 2022, **32**, e00401, DOI: 10.1016/j.susmat.2022.e00401.

11 J. Zhang, J. Anawati and G. Azimi, Urb an mining of terbium, europium, and yttrium from real fluorescent lamp waste using supercritical fluid extraction: Process development and mechanistic investigation, *Waste Manage.*, 2022, **139**, 168–178, DOI: 10.1016/j.wasman.2021.12.033.

12 L. Wang, J. Hou, Y. Chen, B. Tseng and S. Babel, Separation and enrichment of tricolor phosphors in waste phosphors through liquid–liquid–powder extraction method and its benefit evaluation for recovery, *Miner. Eng.*, 2024, **207**, 108572, DOI: 10.1016/j.mineng.2024.108572.

13 J. Lie, H. Shuwanto, H. Abdullah, F. Soetaredjo, S. Ismadji, C. Wijaya and C. Gunarto, Optimization of intensified leaching and selective recovery of Y and Eu from waste cathode ray tube phosphor, *Miner. Eng.*, 2024, **209**, 108620, DOI: 10.1016/j.mineng.2024.108620.

14 O. Artiushenko, W. Rojano, M. Nazarkovsky, M. F. Azevedo, T. Saint'Pierre, J. Kai and V. Zaitsev, Recovery of rare earth elements from waste phosphors using phosphonic acid-functionalized silica adsorbent, *Sep. Purif. Technol.*, 2024, **330**, 125525, DOI: 10.1016/j.seppur.2023.125525.

15 S. Pramanik, A. Kumari, M. Sinha, B. Munshi and S. Sahu, Valorization of phosphor powder of waste fluorescent tubes with an emphasis on the recovery of terbium oxide (Tb4O7), *Sep. Purif. Technol.*, 2023, **322**, 124332, DOI: 10.1016/j.seppur.2023.124332.

16 J. Lie and J. Liu, Recovery of Y and Eu from waste CRT phosphor using closed-vessel microwave leaching, *Sep. Purif. Technol.*, 2021, **277**, 119448, DOI: 10.1016/j.seppur.2021.119448.

17 B. Arunraj, V. Rajesh and N. Rajesh, Potential application of graphene oxide and Aspergillus niger spores with high adsorption capacity for recovery of europium from red phosphor, compact fluorescent lamp and simulated radioactive waste, *J. Rare Earths*, 2021, **41**(1), 157–166, DOI: 10.1016/j.jre.2021.12.006.

18 M. Wu, M. Yu, Q. Cheng, Q. Yuan, G. Mei, Q. Liang and L. Wang, Flotation recovery of Y2O3 from waste phosphors using ionic liquids as collectors, *Chem. Phys. Lett.*, 2023, **825**, 140608, DOI: 10.1016/j.cplett.2023.140608.

19 M. Yamashita, T. Akai, M. Murakami and T. Oki, Recovery of $LaPO_4$:Ce,Tb from waste phosphors using high-gradient magnetic separation, *Waste Manage.*, 2018, **79**, 164–168, DOI: 10.1016/j.wasman.2018.07.038.

20 H. Liu, S. Li, B. Wang, K. Wang, R. Wu, C. Ekberg and A. Volinsky, Multiscale recycling rare earth elements from real waste trichromatic phosphors containing glass, *J. Cleaner Prod.*, 2019, **238**, 117998, DOI: 10.1016/j.jclepro.2019.117998.

21 C. Liu, W. Luo, Y. Li, Z. Wang, S. Xu and X. Wang, Extraction of rare earth Eu from waste blue phosphor strengthened by microwave alkali roasting, *J. Environ. Manage.*, 2024, **362**, 121303, DOI: 10.1016/j.jenvman.2024.121303.

22 S. Back, B. Joung, E. Lee, J. Sung, A. H. M. Mojammal, Y. Park and Y. Seo, Correlation between mercury content and leaching characteristics in waste phosphor powder from spent UV curing lamp after thermal treatment, *J. Hazard. Mater.*, 2020, **382**, 121094, DOI: 10.1016/j.jhazmat.2019.121094.

23 B. Mishra, N. Devi and K. Sarangi, Yttrium and europium recycling from phosphor powder of waste tube light by combined route of hydrometallurgy and chemical reduction, *Miner. Eng.*, 2019, **136**, 43–49, DOI: 10.1016/j.mineng.2019.03.007.

24 Y. Wu, Q. Zhang and T. Zuo, Selective recovery of Y and Eu from rare-earth tricolored phosphorescent powders waste via a combined acid-leaching and photo-reduction process, *J. Cleaner Prod.*, 2019, **226**, 858–865, DOI: 10.1016/j.jclepro.2019.04.137.

25 X. Yin, Y. Wu, L. Wang and T. Zuo, Recovery of Eu from waste blue phosphors ($BaMgAl_{10}O_{17}$: Eu^{2+}) by a sodium peroxide system: Kinetics and mechanism aspects, *Miner. Eng.*, 2020, **151**, 106333, DOI: 10.1016/j.mineng.2020.106333.

26 Y. Wu, B. Wang, Q. Zhang, R. Li and J. Yu, A novel process for high efficiency recovery of rare earth metals from waste phosphors using a sodium peroxide system, *RSC Adv.*, 2014, **4**, 7927–7932, DOI: 10.1039/c3ra46381h.

27 X. Yin, X. Tian, Y. Wu, Q. Zhang, W. Wang, B. Li, Y. Gong and T. Zuo, Recycling rare earth elements from waste cathode ray tube phosphors: Experimental study and mechanism analysis, *J. Cleaner Prod.*, 2018, **205**, 58–66, DOI: 10.1016/j.jclepro.2018.09.055.

28 Y. Liang, Y. Liu, R. Lin, D. Guo and C. Liao, Leaching of rare earth elements from waste lamp phosphor mixtures by reduced alkali fusion followed by acid leaching, *Hydrometallurgy*, 2016, **163**, 99–103, DOI: 10.1016/j.hydromet.2016.03.020.

29 B. Xie, C. Liu, B. Wei, R. Wang and R. Ren, Recovery of rare earth elements from waste phosphors via alkali fusion roasting and controlled potential reduction leaching, *Waste Manage.*, 2023, **163**, 43–51, DOI: 10.1016/j.wasman.2023.03.029.

30 F. Zhu, P. Zhang, G. Gao, Z. Ma, T. Mu, J. Li and K. Qiu, Efficient preparation of metallic titanium from lower valence titanium chloride slurry by electrochemical reduction in molten salts, *J. Environ. Chem. Eng.*, 2024, **12**(3), 112983, DOI: 10.1016/j.jece.2024.112983.

31 Q. Meng, Y. Zhang, P. Dong and F. Liang, A novel process for leaching of metals from $LiNi_{1/3}Co_{1/3}Mn_{1/3}O_2$ material of spent lithium ion batteries: Process optimization and kinetics aspects, *J. Ind. Eng. Chem.*, 2018, **61**, 133–141, DOI: 10.1016/j.jiec.2017.12.010.

32 Q. Meng, Y. Zhang and P. Dong, Use of electrochemical cathode-reduction method for leaching of cobalt from spent lithium-ion batteries, *J. Cleaner Prod.*, 2018, **180**, 64–70, DOI: 10.1016/j.jclepro.2018.01.101.

33 J. Yang, Y. Zhou, Z. Zhang, K. Xu, K. Zhang, Y. Lai and L. Jiang, Effect of electric field on leaching valuable metals from spent lithium-ion batteries, *Trans. Nonferrous Met. Soc. China*, 2023, **33**, 632–641, DOI: 10.1016/S1003-6326(22)66134-X.